(Received 6 November 2024, Accepted 17 December 2024, Scheduled 26 December 2024)

A Defective Ground Structure Design for Reducing Coupling between Microstrip Antenna Arrays

Junhao Xu[1, 2], Yafei Wang[1, 2, *], Xiaozhe Wang[1, 2], and Zhensong Li[1, 2]

[1] *Key Laboratory of Information and Communication Systems, Ministry of Information Industry, Beijing Information Science and Technology University, Beijing 100101, China*
[2] *Key Laboratory of Modern Measurement & Control Technology, Ministry of Education, Beijing Information Science and Technology University, Beijing 100101, China*

ABSTRACT: In order to reduce the coupling between dense antenna arrays in multiple input multiple output (MIMO) systems, this paper proposes a method to reduce the coupling between microstrip antenna arrays by utilizing a defected ground structure (DGS), which consists of "W"-shaped slits etched in the ground plane. Simulation results show that the structure can achieve -46.6 dB isolation between antenna arrays. To verify the effectiveness of the structure, the microstrip antenna arrays loaded with this DGS are fabricated and measured, and the measured results are consistent with the simulated ones, which verifies the effectiveness of the structure.

1. INTRODUCTION

With the rapid development of mobile communication technology, MIMO has become a research hotspot in wireless communication because of its advantages of high-speed rate, large capacity, high transmission reliability, etc. [1]. MIMO refers to the use of multiple antennas for synchronous transmitting and receiving at both the transmitter and receiver ends of a wireless network system, as a way to increase the transmission rate of information and system capacity. However, with the development of mobile terminal equipment towards miniaturization, multiple antenna elements have to be placed in a limited space. When the spacing of the antenna elements is low, a strong coupling effect occurs which seriously affects the radiation characteristics of the antenna.

Electromagnetic coupling refers to interactions between two or more circuit elements that result in energy transfer between the circuit elements. The coupling between antenna arrays can be classified into two types. The first type of coupling originates from the antenna ground or surface waves. In this case, the signal propagates from the feed port to other ports in the form of current or surface waves, causing interference. The second type is radiative coupling from the surrounding transmission space. Not all electromagnetic waves emitted by the feed antenna reach the target antenna. Some of these waves are received by adjacent antennas, resulting in coupling interference between the two elements [2]. Strong coupling effects lead to reduced antenna radiation efficiency, gain reduction, poor impedance matching characteristics, and distortion of the far-field radiation pattern so reducing the coupling between antenna arrays is very important in MIMO systems.

Researchers have proposed various methods to reduce the coupling between microstrip antenna arrays without changing the microstrip antenna arrays spacing. In particular, electromagnetic bandgap (EBG) technique and DGS technique have attracted widespread attention. EBG technique consists of through-hole structures periodically arranged between antenna arrays, which can effectively suppress mutual coupling. However, the large antenna arrays spacing requirement and high manufacturing cost hinder the application of this technique in compact microstrip antennas. The DGS technique consists of etching differently shaped slots in the ground plane of the antenna array without any additional structure. DGS can be viewed as a high-impedance band-stop filter that isolates the scattered currents between antenna arrays. In comparison, DGS technique does not require a large antenna arrays spacing and is simple to fabricate. An S-shaped periodic DGS is proposed, aiming to reduce the coupling between coplanar antenna arrays. This structure can effectively reduce the coupling between coplanar antenna arrays [3]. A DGS of meandered lines is proposed to reduce the mutual coupling between two microstrip antennas. The proposed structure is optimized and explained by the common/differential mode theory. This structure significantly reduces coupling and improves radiation efficiency and gain [4]. A novel T-shaped DGS is presented to reduce the mutual coupling between dual feed points circularly polarized microstrip antennas. This structure can reduce the coupling between the same polarization ports in parallel and series arrangements, improving the radiation efficiency and gain [5]. A surrogate-assisted DGS design is proposed to suppress E-plane and H-plane couplings. The DGS is designed and analyzed based on the magnetic current and mode theory. Machine learning is used to optimize the DGS parameters. This structure can reduce the coupling in the E-plane and H-plane and improve the radiation efficiency and gain [6]. Although these mentioned papers have made improvements at different levels in the decoupling effect, there is still potential for fur-

* Corresponding author: Yafei Wang (wangyafei@bistu.edu.cn).

ther reductions in the decoupling effect, DGS complexity, and spacing of the antenna arrays.

Based on the S-shaped DGS, this paper designs a more simple and compact W-shaped DGS. Under the premise of ensuring the stability of the physical characteristics of the antenna, the structure can effectively suppress the coupling between the antenna arrays. The microstrip line loaded with the DGS and its corresponding equivalent circuit are constructed, and the parameters of this DGS are analyzed. Using high frequency simulator structure (HFSS) software, the rules of the variation in the parameter dimensions of the DGS were analyzed. Moreover, the S-parameters, envelope correlation coefficient, and far-field radiation gain are compared before and after the antenna array was loaded with a W-shaped DGS. The simulation and measurement results show that the isolation degree of the antenna at the center frequency can be increased by 46.6 dB after loading the W-shaped DGS, which verifies the effectiveness of the structure.

2. W-SHAPED DGS AND CHARACTERIZATION

To analyze the characteristics of the W-shaped DGS, a microstrip line loaded with the DGS is established as shown in Fig. 1 where the upper layer of the dielectric substrate is a microstrip transmission line with a characteristic impedance of 50 Ω, and the W-shaped DGS is etched in the ground plane.

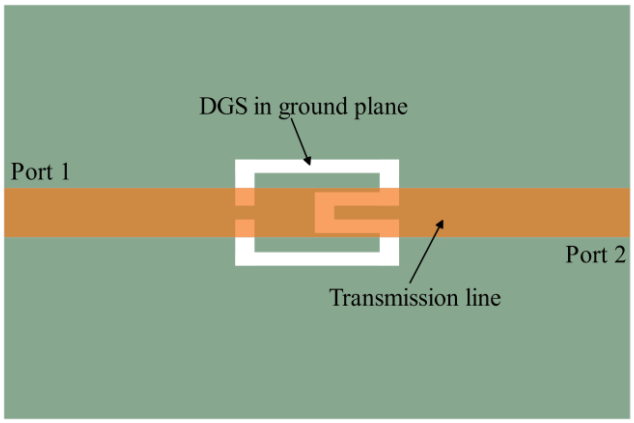

FIGURE 1. Microstrip line loaded with W-shaped DGS.

By using the HFSS software, the effects of the structural parameters of the W-shaped DGS on the frequency response characteristics of the microstrip line are analyzed. The substrate is Rogers 5880 with a dielectric constant $\varepsilon_r = 2.2$ and thickness of $h = 1.5$ mm. The planar structure of the DGS is shown in Fig. 2, where the main parameters of the DGS are L_1, L_2, L_5, and g. Firstly, the effects of L_1 and L_2 on the frequency response characteristics of the microstrip line are analyzed, and the simulation results are shown in Figs. 4 and 5. As L_1 and L_2 become larger, the -3 dB cutoff frequency and attenuation pole frequency become significantly smaller, which indicates that L_1 and L_2 affect the -3 dB cutoff frequency and attenuation pole frequency simultaneously.

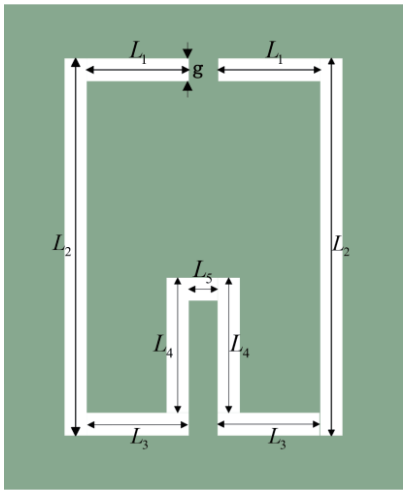

FIGURE 2. W-shaped DGS planar structure.

Then the effects of L_5 and g on the frequency response characteristics of the microstrip line are analyzed, and the simulation results are shown in Figs. 6 and 7. As L_5 and g become larger, the attenuation pole moves to the high frequency, while the -3 dB cutoff frequency is almost unchanged. It can be seen that the larger the L_5 and g are, the larger the attenuation pole is; L_5 and g do not affect the -3 dB cutoff frequency. From the above, it can be concluded that the cutoff frequency mainly depends on the parameters L_1 and L_2; the attenuation pole depends on the parameters L_1, L_2, L_5, and g.

DGS affects the distribution of the equivalent capacitance and inductance of the microstrip line through the introduction of slits, so the DGS can be analyzed with an RLC circuit [7]. In the following, the equivalent circuit model of the microstrip line loaded with the DGS will be constructed, and the circuit parameters will be extracted and verified. Fig. 8 shows the corresponding RLC circuit of the microstrip line loaded with the DGS. Formulas (1) and (2) represent the equivalent capacitance C and equivalent inductance L, respectively, based on the RLC

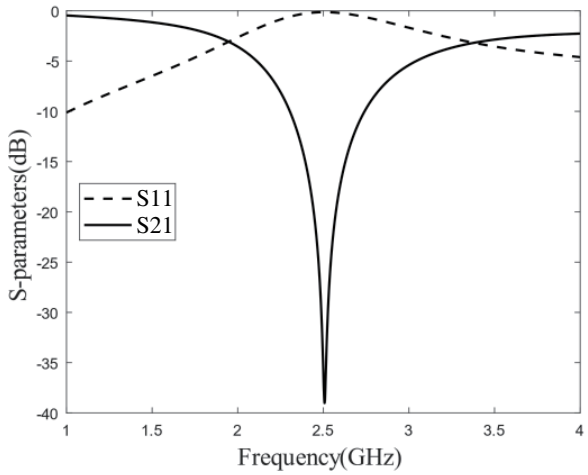

FIGURE 3. Frequency response characteristic curves of the microstrip line loaded with W-shaped DGS.

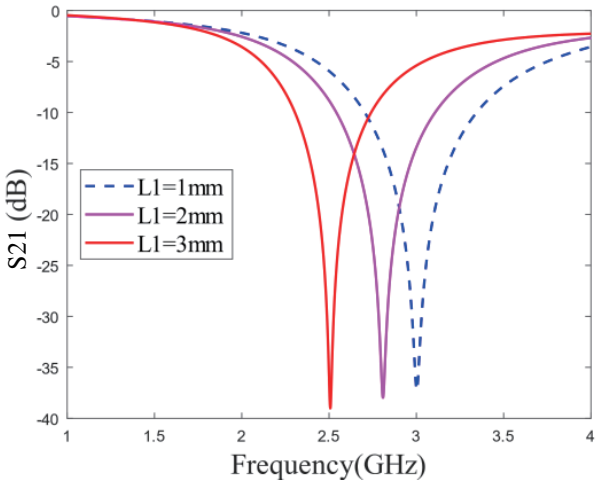

FIGURE 4. Trend of frequency response characteristics of the microstrip line with parameter L_1.

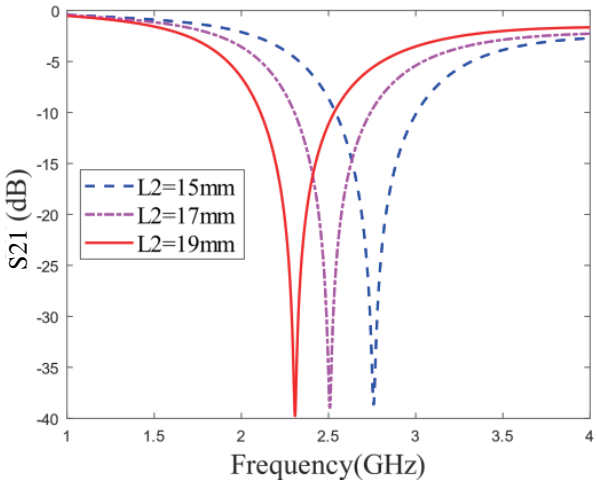

FIGURE 5. Trend of frequency response characteristics of the microstrip line with parameter L_2.

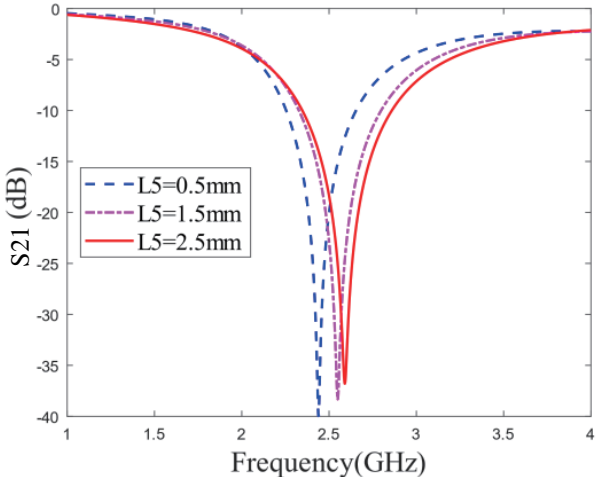

FIGURE 6. Trend of frequency response characteristics of the microstrip line with parameter L_5.

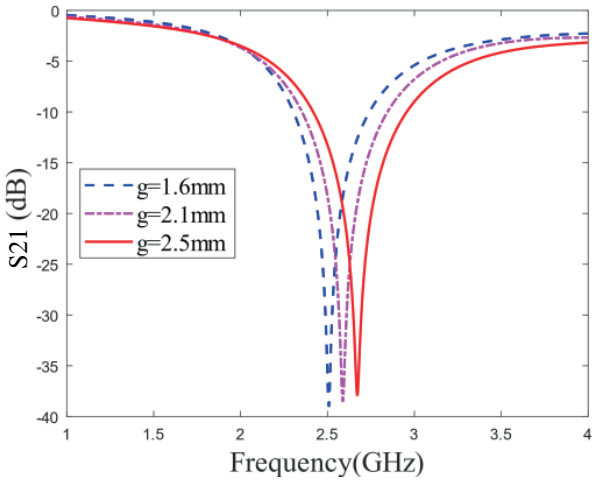

FIGURE 7. Trend of frequency response characteristics of the microstrip line with parameter g.

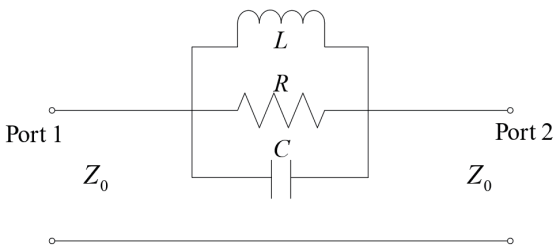

FIGURE 8. Equivalent circuit of a microstrip line loaded with W-shaped DGS.

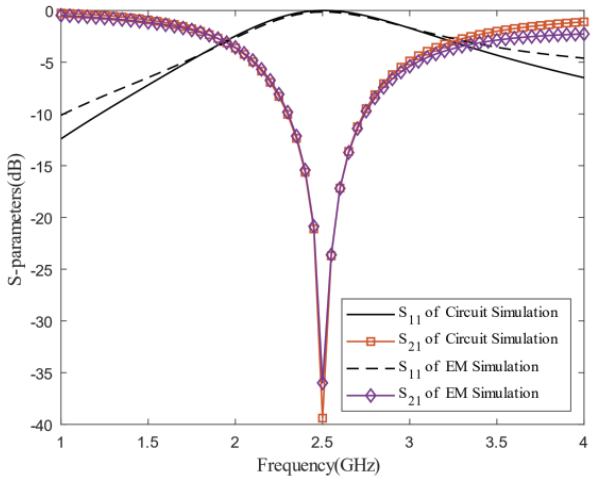

FIGURE 9. Comparing the frequency response characteristic curves of microstrip lines and equivalent circuits.

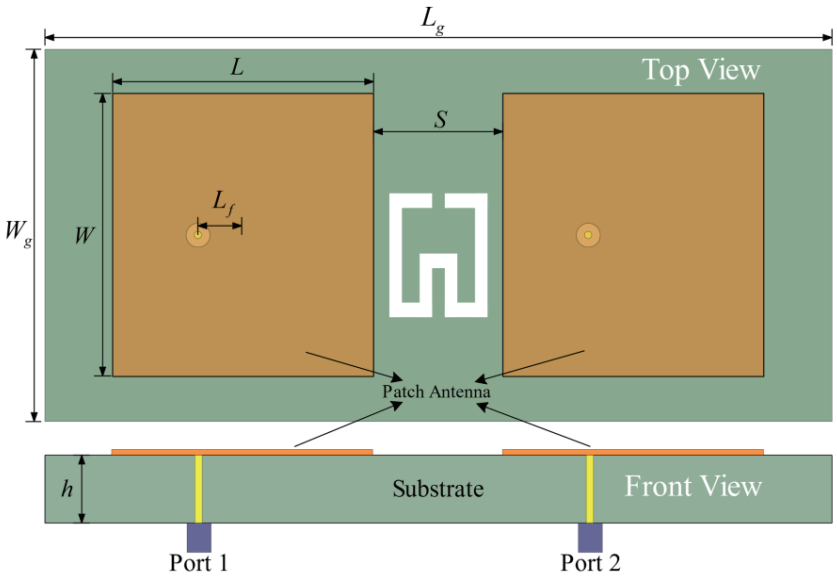

FIGURE 10. Microstrip antenna arrays.

oscillating circuit's operating principle [8].

$$C = \frac{\omega_c}{2Z_0(\omega_0^2 - \omega_c^2)} \tag{1}$$

$$L = \frac{1}{4\pi^2 f_0^2 C} \tag{2}$$

where Z_0 is the characteristic impedance of the microstrip line ω_0 the resonant corner frequency, ω_c the -3 dB cutoff corner frequency, and f_0 the resonant center frequency.

As depicted in Fig. 3, the aforementioned required data can be acquired. Subsequently, by performing calculations based on Formula (1), it is obtained that the equivalent capacitance $C = 1.219$ pF. Substituting $f_0 = 2.5$ GHz and the $C = 1.219$ pF into Formula (2), it is obtained that the equivalent inductance $L = 3.304$ nH. From the above calculations, the values of C and L in Fig. 8 can be assigned. The frequency response characteristics of this circuit are analyzed through advanced design system (ADS) software. The circuit frequency response characteristic curve calculated by ADS software is compared with the microstrip line frequency response characteristic curve calculated by HFSS software. As shown in Fig. 9, the -3 dB cutoff frequency of the circuit $f_c = 1.9$ GHz, the resonant center frequency $f_0 = 2.5$ GHz, and the magnitude of S_{21} is -39 dB at 2.5 GHz. This is basically consistent with the microstrip line frequency response characteristic curve calculated by HFSS.

According to the frequency response characteristic curve of the microstrip line loaded with the W-shaped DGS, it is seen that the transmission coefficient S_{21} has an obvious band-stop filtering characteristic at 2.5 GHz, which indicates that the electromagnetic energy is not transmitted to the other port through the microstrip line. It has been verified that the W-shaped DGS can effectively suppress the transmission of electromagnetic energy within a certain frequency band. Evidently, by loading the optimized W-shaped DGS between antenna arrays, the coupling between the antenna arrays can be reduced.

3. ANTENNA DECOUPLING DESIGN

The spacing of microstrip antenna arrays is usually designed to be more compact to accommodate the trend of increasing miniaturization of mobile communication terminal devices [9]. However, excessively small spacing will cause coupling between the antennas. To minimize the coupling, the W-shaped DGS designed in the previous section can be loaded to the ground plane of the microstrip antenna arrays. The microstrip antenna arrays loaded with a W-shaped DGS are shown in Fig. 10.

In the figure, two rectangular patches are placed side by side on the upper layer of the dielectric substrate, with the dimensions of $W \times L$, and the antenna arrays spacing is S (about $0.16\lambda_0$, where λ_0 is the free-space wavelength at 2.5 GHz); the dielectric substrate is made of F4B, with a dielectric constant $\varepsilon_r = 2.2$ and thickness of $h = 3$ mm; the dimensions of both the dielectric substrate and ground plane are $W_g \times L_g$; the antenna is fed by a coaxial feed, and the spacing from the center of feed to the center of the rectangular patche is L_f. The size of the inner core of the feed is $R = 0.7$ mm, which provides 50 Ω matching impedance; the central operating frequency of the antenna is 2.5 GHz; the parameter scanning analysis of the antenna is carried out by using HFSS. Table 1 presents the optimal dimensions of the antenna arrays loaded with the W-shaped DGS.

4. EXPERIMENTAL AND MEASUREMENT RESULTS

To verify the effectiveness of the W-shaped DGS on the coupling suppression between the microstrip antenna arrays, the

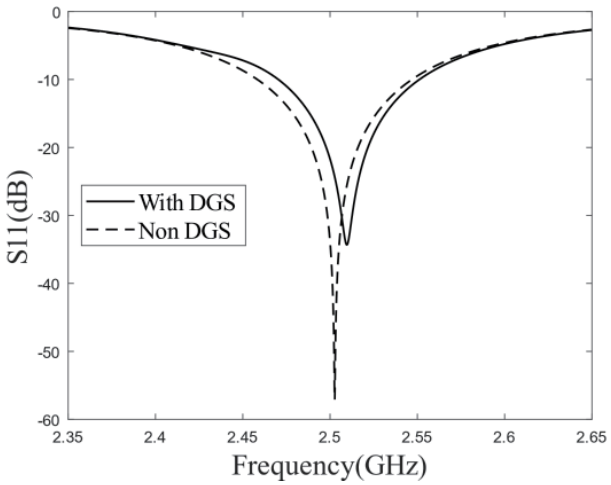

FIGURE 11. S_{11} of microstrip antenna arrays with and without loading W-shaped DGS.

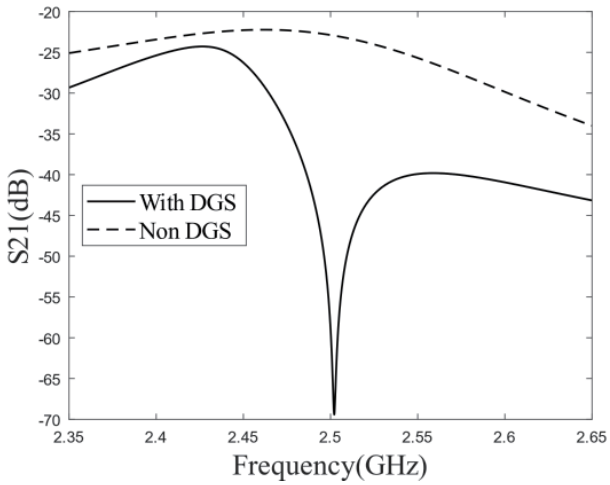

FIGURE 12. S_{21} of microstrip antenna arrays with and without loading W-shaped DGS.

proposed microstrip antenna arrays loaded with W-shaped DGS are simulated with HFSS software. The dimensions of the W-shaped DGS and the microstrip antennas are given in Table 1. The simulation frequency is set from 2.35 GHz to 2.65 GHz, and the simulation results include S-parameters, envelope correlation coefficients, and far-field radiation pattern.

TABLE 1. Antenna arrays and W-shaped DGS dimensions.

	W	L	W_g	L_g	L_f	g
Parameters (mm)	38.3	37.1	50	112	6.8	2
	L_1	L_2	L_3	L_4	L_5	
	4.2	16.7	4.2	5.6	2	

4.1. S-Parameter

The performance of the antenna can be evaluated by S_{11} and S_{21}, where S_{11} is the reflection coefficient of the antenna port, indicating the amount of energy reflected from the antenna port; S_{21} is the coupling coefficient from the first antenna to the second antenna, which is numerically equal to the ratio of the signal power between the second antenna port and the first antenna port. A smaller value of S_{21} indicates a lower coupling between the two antennas [10].

The resonant frequency of the antenna is defined as the frequency range within which the antenna meets the operational requirements and thus realizes the effective reception and transmission of the signal. For the antenna, the resonant frequency is defined as the frequency range in which the reflection coefficient S_{11} of the antenna is below -10 dB. The center frequency of the antenna is defined as the frequency corresponding to the lowest S_{11} in the resonant frequency range, and the gain and efficiency of the antenna reach the maximum value at the center frequency.

The simulation results of the S-parameters obtained for the microstrip antenna arrays with and without loading the W-shaped DGS are shown in Figs. 11 and 12, respectively. It can be seen that the S_{21} of the microstrip antenna without loading the DGS is -22.8 dB, whereas the S_{21} of the microstrip antenna with loading the W-shaped DGS is -69.4 dB, which indicates that loading the DGS can effectively reduce the coupling between the antenna arrays by 46.6 dB. After adding the DGS, the center resonant frequency of the antenna arrays is moved from the initial 2.5 GHz to the high frequency direction by 10 MHz, so in the design of antenna arrays, to make sure that the antenna arrays operating in the necessary frequency band, the effects of the patch dimension and the DGS on the antenna's center resonant frequency must be considered and modified.

4.2. Correlation Coefficient

The spatial correlation of the signal is a key factor affecting the performance of the MIMO systems. The spatial correlation of the antenna refers to the correlation characteristics between the antenna at the transmitting end and the antenna at the receiving end, which is generally expressed by the correlation coefficient. If the correlation coefficient is too large, the channel capacity of the MIMO systems will be significantly lost. In order to achieve good performance, a necessary condition is to have a low correlation between the transmitter and receiver antennas.

The correlation between the envelopes of two signals is known as the envelope correlation coefficient (ECC), and it is calculated by Formula (3):

$$\rho_e = \frac{E\left\{\left(|x_1|^2 - E\left\{|x_1|^2\right\}\right)\left(|x_2|^2 - E\left\{|x_2|^2\right\}\right)^*\right\}}{\sqrt{E\left\{\left||x_1|^2 - E\left\{|x_1|^2\right\}\right|^2\right\} E\left\{\left||x_2|^2 - E\left\{|x_2|^2\right\}\right|^2\right\}}} \tag{3}$$

where x_1 and x_2 represent the two shunt signals, respectively. $E\{\cdot\}$ represents the expected value of the signal. ρ_e is the ECC of the antenna

According to HFSS, the correlation coefficients of antennas with and without loading the W-shaped DGS are shown

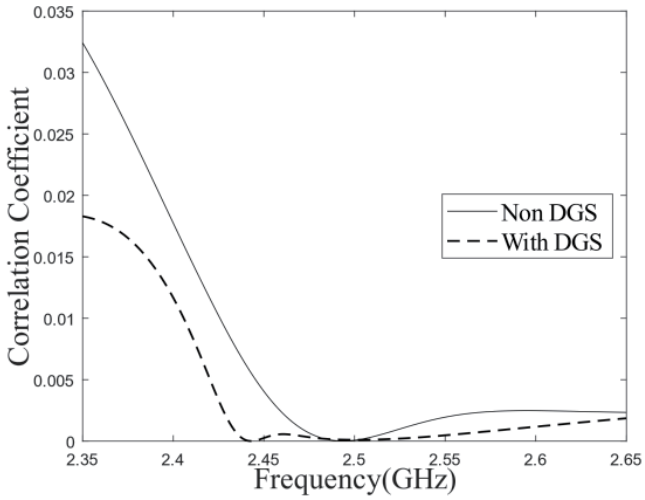

FIGURE 13. Correlation coefficients of microstrip antenna arrays with and without loading W-shaped DGS.

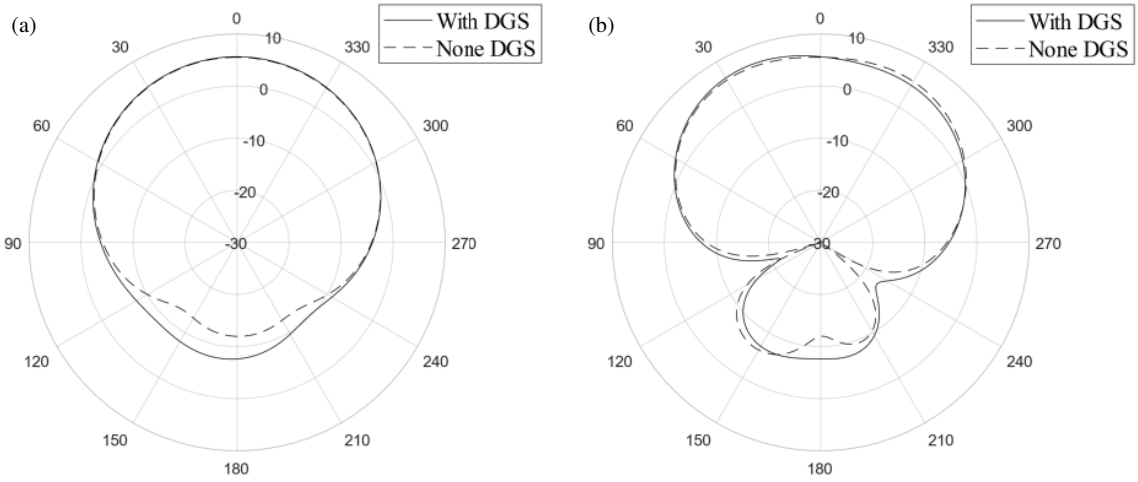

FIGURE 14. Far-field radiation pattern of microstrip antenna arrays with and without loading DGS. (a) E-plane. (b) H-plane.

in Fig. 13. The figure shows that the overall envelope correlation coefficient is less than 0.018, which indicates that adding this structure makes the correlation coefficient between the two antennas significantly lower, demonstrating that the loading of the structure significantly improves the isolation between the antennas.

4.3. Far-Field Radiation Pattern

Figure 14 shows the radiation patterns in the E-plane and H-plane of the microstrip antenna arrays with and without loading the W-shaped DGS. The gain patterns of the antennas exhibit directional radiation characteristics. After the DGS is loaded, the forward radiation patterns in both the E-plane and H-plane remain unchanged, while the backward radiation of the antenna increases by up to 4.33 dB. This increase is due to a portion of the antenna's energy being radiated into free space through the DGS [11]. The results show that the W-shaped DGS has almost no impact on the radiation pattern while the isolation between antenna arrays is significantly improved.

To further validate the effect of the proposed W-shaped DGS on reducing the coupling between the microstrip antenna arrays, the microstrip antenna arrays loaded with the W-shaped DGS were processed and measured by a vector network analyzer. The prototype of the antenna arrays was fabricated according to the parameters in Table 1, as shown in Fig. 15. Fig. 15(a) shows the top view of the antenna arrays, and Fig. 15(b) shows the bottom view of the antenna arrays

Figure 16 shows the comparison curves between simulated and measured S_{11} and S_{21} parameters. The measurement results indicate that the bandwidth is 80.8 MHz with $S_{11} < -10$ dB (ranging from 2.4704 to 2.5512 GHz). The center frequency of S_{21} is 2.5021 GHz, and the coupling between the antenna arrays has decreased from -22 dB to -63 dB, achieving a coupling suppression of 41 dB. Overall, the measured results are in good agreement with the simulated ones.

TABLE 2. Comparison of antenna performance with existing papers.

Design technique	Resonant frequency	Edge to edge distance	Reduced coupling	Complexity
Reference [2]	2.57 GHz	$0.17\lambda_0$	40 dB	medium
Reference [4]	2.48 GHz	$0.38\lambda_0$	42 dB	High
Reference [6]	2.45 GHz	$0.37\lambda_0$	27 dB	medium
Reference [11]	2.4 GHz	$0.37\lambda_0$	10 dB	Low
Present work	2.5 GHz	$0.16\lambda_0$	46 dB	Low

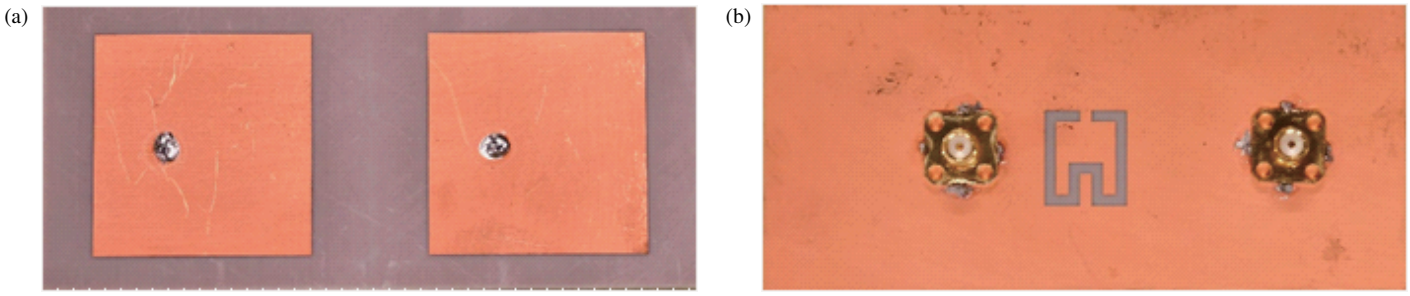

FIGURE 15. The prototype of microstrip antenna arrays with W-shaped DGS. (a) Top view. (b) Bottom view.

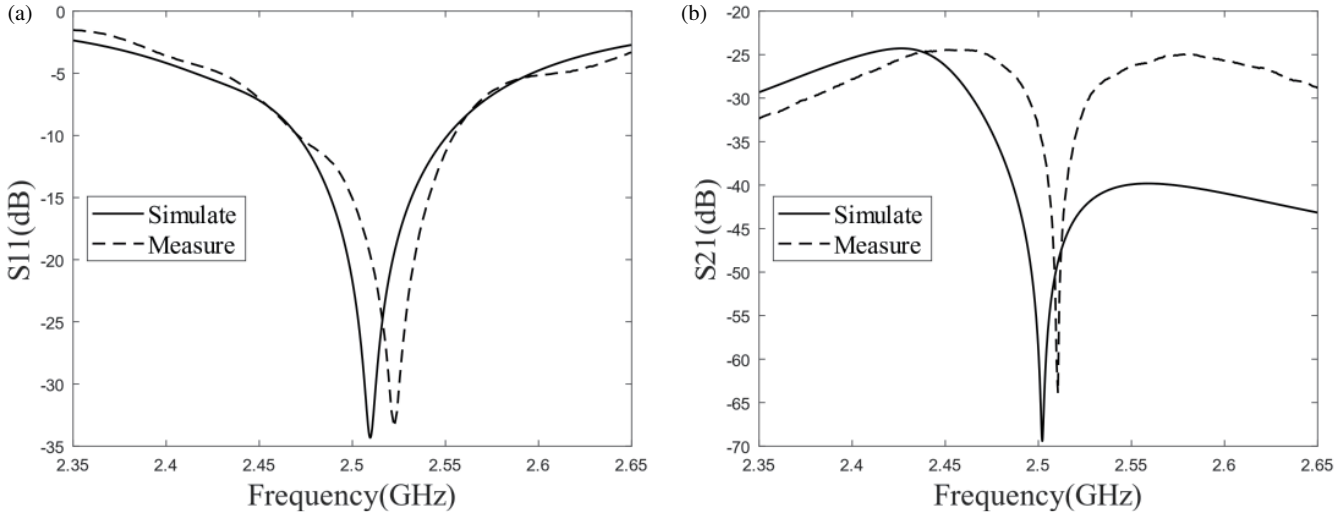

FIGURE 16. Simulation and measurement comparison curves for S_{11} and S_{21} of the antenna arrays. (a) Simulation and measurement comparison curves for S_{11} of the antenna arrays. (b) Simulation and measurement comparison curves for S_{21} of the antenna arrays.

Meanwhile, the method of this paper was compared with other methods, and the comparison results are shown in Table 2. The decoupling effect and structural complexity of the W-shaped DGS designed in this paper are better than other structures.

5. CONCLUSION

In order to suppress the coupling between microstrip antenna arrays, a simple and compact W-shaped DGS is designed in this paper. Firstly, a W-shaped DGS is etched in the ground plane of the microstrip line. Then, the band-resistance characteristics of the structure are analyzed, and the equivalent circuit is extracted. Subsequently, the dimensions of the W-shaped DGS are optimized, and then the DGS is loaded on the microstrip antenna arrays. The addition of W-shaped DGS reduces the coupling between the antenna arrays by a maximum of 46.6 dB, and a comparative analysis is conducted with other papers. The results indicate that when the spacing is $0.16\lambda_0$, the W-shaped DGS exhibits advantages compared to other structures with regard to the decoupling effect and structural complexity. The simulated and measured results demonstrate that the addition of the W-shaped DGS effectively suppresses the coupling between the antenna arrays, thus providing an effective solution for reducing the coupling between microstrip antenna arrays and enhancing the performance of MIMO systems.

ACKNOWLEDGEMENT

The Joint Funds of the National Natural Science Foundation of China (Ye Qisun Science Foundation) under Grant U2341223.

REFERENCES

[1] Fang, Y., Y. Liu, Y. Jia, J. Liang, and H. H. Zhang, "Reconfigurable structure reutilization low-SAR MIMO antenna for 4G/5G full-screen metal-frame smartphone operation," *IEEE Antennas and Wireless Propagation Letters*, Vol. 22, No. 5, 1219–1223, 2023.

[2] Zhang, H., Y. Wang, and X. Li, "A method of reducing coupling between PIFA antennas using cross slot defected ground structure," *Progress In Electromagnetics Research M*, Vol. 124, 1–9, 2024.

[3] Wei, K., J. Li, L. Wang, Z. Xing, and R. Xu, "S-shaped periodic defected ground structures to reduce microstrip antenna array mutual coupling," *Electronics Letters*, Vol. 52, No. 15, 1288–1290, 2016.

[4] Qian, B., X. Chen, and A. A. Kishk, "Decoupling of microstrip antennas with defected ground structure using the common/differential mode theory," *IEEE Antennas and Wireless Propagation Letters*, Vol. 20, No. 5, 828–832, 2021.

[5] Li, Z.-L., Z.-J. Xing, and J.-Y. Li, "A T-shaped defected ground structure for decoupling circularly polarization microstrip antenna array," in *2021 IEEE International Symposium on Antennas and Propagation and USNC-URSI Radio Science Meeting (APS/URSI)*, 933–934, Singapore, Dec. 2021.

[6] Qian, B., X. Huang, X. Chen, M. Abdullah, L. Zhao, and A. A. Kishk, "Surrogate-assisted defected ground structure design for reducing mutual coupling in 2 × 2 microstrip antenna array," *IEEE Antennas and Wireless Propagation Letters*, Vol. 21, No. 2, 351–355, 2021.

[7] Gao, D., Z.-X. Cao, S.-D. Fu, X. Quan, and P. Chen, "A novel slot-array defected ground structure for decoupling microstrip antenna array," *IEEE Transactions on Antennas and Propagation*, Vol. 68, No. 10, 7027–7038, 2020.

[8] Wei, K., "Defected ground structure for suppressing mutual coupling and achieving antenna circular polarization," Ph.D. dissertation, Northwestern Polytechnical University, XiAn, China, 2017.

[9] Acharjee, J., K. Mandal, S. K. Mandal, and P. P. Sarkar, "Mutual coupling reduction between microstrip patch antennas by using a string of H-shaped DGS," in *2016 International Conference on Microelectronics, Computing and Communications (MicroCom)*, 1–3, Durgapur, India, Jan. 2016.

[10] Qian, B. and X. Chen, "Mutual coupling reduction in 4 × 4 microstrip array using H-shaped defected ground structure," in *2022 International Conference on Microwave and Millimeter Wave Technology (ICMMT)*, 1–3, Harbin, China, Aug. 2022.

[11] Pasha, M. I., C. Kumar, and D. Guha, "Simultaneous compensation of microstrip feed and patch by defected ground structure for reduced cross-polarized radiation," *IEEE Transactions on Antennas and Propagation*, Vol. 66, No. 12, 7348–7352, 2018.